The Astrophysical Journal, 645:L89–L92, 2006 July 10

A BLIND ESTIMATION OF THE ANGULAR POWER SPECTRUM OF CMB ANISOTROPY FROM *WMAP*

Rajib Saha,[1,2] Pankaj Jain,[1] and Tarun Souradeep[2]

Received 2005 October 26; accepted 2006 May 31; published 2006 July 11

ABSTRACT

Accurate measurements of the angular power spectrum of cosmic microwave background (CMB) radiation have lead to a marked improvement in the estimates of different cosmological parameters. This has required removal of foreground contamination as well as detector noise bias with reliability and precision. We present the estimation of the CMB angular power spectrum from the multifrequency observations of the *Wilkinson Microwave Anisotropy Probe* (*WMAP*) using a novel *model-independent* method. The primary results of *WMAP* are the observations of the CMB in 10 independent difference assemblies (DAs) that have uncorrelated noise. Our method utilizes the maximum information available within the *WMAP* data by linearly combining all the DA maps in order to remove foreground contamination and by estimating the power spectrum from cross-power spectra of clean maps with independent noise. We compute 24 cross-power spectra that are the basis of the final power spectrum. The binned average power matches the *WMAP* team's published power spectrum closely. A small systematic difference at large multipoles is accounted for by the correction for the expected residual power from unresolved point sources. The correction is small and significantly tempered. Previous estimates have depended on foreground templates built using extraneous observational input. This is the *first demonstration that the CMB angular spectrum can be reliably estimated with precision from a self-contained analysis of the WMAP data*.

Subject headings: cosmic microwave background — cosmology: observations

Online material: color figures

1. INTRODUCTION

Remarkable progress in cosmology has been made due to the measurements of the anisotropy in the cosmic microwave background (CMB) over the past decade. The extraction of the angular power spectrum of the CMB anisotropy is complicated by foreground emission within our Galaxy and from extragalactic radio sources, as well as by detector noise (Bouchet & Gispert 1999; Tegmark & Efstathiou 1996). It is established that the CMB follows a blackbody distribution to high accuracy (Mather et al. 1994, 1999). Hence, foreground emissions may be removed by exploiting the fact that their contributions to different spectral bands are considerably different while the CMB power spectrum is the same in all the bands (Dodelson 1997; Tegmark et al. 2000; Bennett et al. 2003b; Tegmark 1998). Different approaches to foreground removal have been proposed in the literature (Bouchet & Gispert 1999; Tegmark & Efstathiou 1996; Hobson et al. 1998; Maino et al. 2002, 2003; Eriksen et al. 2006).

The *Wilkinson Microwave Anisotropy Probe* (*WMAP*) observes in five frequency bands at 23 GHz (K), 33 GHz (Ka), 41 GHz (Q), 61 GHz (V), and 94 GHz (W). In the first data release, the *WMAP* team removed the Galactic foreground signal using a template-fitting method based on a model of synchrotron, free-free, and dust emission in our Galaxy (Bennett et al. 2003b). The sky maps around the Galactic plane and around known extragalactic point sources were masked out, and the CMB power spectrum was then obtained from cross-power spectra of independent difference assemblies in the 41, 61, and 94 GHz foreground-cleaned maps (Hinshaw et al. 2003b).

A model-independent removal of foregrounds has been proposed in the literature (Tegmark & Efstathiou 1996). The method has also been used on the *WMAP* data in order to create a foreground-cleaned map (Tegmark et al. 2003). The main advantage of this method is that it does not make any additional assumptions regarding the nature of the foregrounds. Furthermore, the procedure is computationally fast. The foreground emissions are removed by combining the five different *WMAP* bands by weights that depend both on the angular scale and on the location in the sky (divided into regions based on "cleanliness"). However, this analysis did not attempt to remove the detector noise bias (Tegmark et al. 2003). Consequently, the power spectrum recovered from the foreground-cleaned map has a lot of excess power at large multipole moments due to amplification of detector noise bias beyond the beam resolution.

The prime objective of our Letter is to remove detector noise bias by exploiting the fact that it is uncorrelated among the different difference assemblies (DAs; Hinshaw et al. 2003b; Jarosik et al. 2003). The *WMAP* data use 10 DAs (Bennett et al. 2003a, 2003c; Limon et al. 2003; Hinshaw et al. 2003a), one each for K and Ka bands, two for the Q band, two for the V band, and four for the W band. We label these K, Ka, Q1, Q2,V1, V2, W1, W2, W3, and W4, respectively. We eliminate the detector noise bias by using cross-power spectra, and we provide a model-independent extraction of the CMB power spectrum from *WMAP* first-year data. So far, only the three highest frequency channels observed by *WMAP* have been used to extract the CMB power spectrum, and the foreground removal required foreground templates based on extrapolated flux from measurements at frequencies far removed from the observational frequencies of *WMAP* (Hinshaw et al. 2003b; Fosalba & Szapudi 2004; Patanchon et al. 2005). We present a more general procedure, in which we use observations from all five frequency channels of *WMAP*, and we do not use any extraneous observational input.

2. METHODOLOGY

2.1. *Foreground Cleaning*

Up to the foreground cleaning stage, our method is similar to that of Tegmark & Efstathiou (1996) and Tegmark et al.

[1] Physics Department, Indian Institute of Technology, Kanpur, UP 208016, India.

[2] Inter-University Centre for Astronomy and Astrophysics (IUCAA), Post Bag 4, Ganeshkhind, Pune 411007, India.

TABLE 1
DIFFERENT COMBINATIONS OF THE DA MAPS USED TO OBTAIN THE FINAL 48 CLEANED MAPS

(K, Ka) + Q1 + V1 +W12 = (C1, CA1)	(K, Ka) + Q1 + V2 + W12 = (C13, CA13)
(K, Ka) + Q1 + V1 + W13 = (C2, CA2)	(K, Ka) + Q1 + V2 + W13 = (C14, CA14)
(K, Ka) + Q1 + V1 + W14 = (C3, CA3)	(K, Ka) + Q1 + V2 + W14 = (C15, CA15)
(K, Ka) + Q1 + V1 + W23 = (C4, CA4)	(K, Ka) + Q1 + V2 + W23 = (C16, CA16)
(K, Ka) + Q1 + V1 + W24 = (C5, CA5)	(K, Ka) + Q1 + V2 + W24 = (C17, CA17)
(K, Ka) + Q1 + V1 + W34 = (C6, CA6)	(K, Ka) + Q1 + V2 + W34 = (C18, CA18)
(K, Ka) + Q2 + V2 + W12 = (C7, CA7)	(K, Ka) + Q2 + V1 + W12 = (C19, CA19)
(K, Ka) + Q2 + V2 + W13 = (C8, CA8)	(K, Ka) + Q2 + V1 + W13 = (C20, CA20)
(K, Ka) + Q2 + V2 + W14 = (C9, CA9)	(K, Ka) + Q2 + V1 + W14 = (C21, CA21)
(K, Ka) + Q2 + V2 + W23 = (C10, CA10)	(K, Ka) + Q2 + V1 + W23 = (C22, CA22)
(K, Ka) + Q2 + V2 + W24 = (C11, CA11)	(K, Ka) + Q2 + V1 + W24 = (C23, CA23)
(K, Ka) + Q2 + V2 + W34 = (C12, CA12)	(K, Ka) + Q2 + V1 + W34 = (C24, CA24)

(2003). In Tegmark et al. (2003), a foreground-cleaned map is obtained by linearly combining five maps that correspond to each of the different *WMAP* frequency channels. For the Q, V, and W frequency channels, for which more than one map was available, an averaged map was used. However, averaging over the DA maps in a given frequency channel precludes any possibility of removing detector noise bias using cross-correlation. In our method, we linearly combine maps corresponding to a set of four DA maps at different frequencies. We treat the K and Ka maps effectively as the observation of the CMB in two different DAs. Therefore, we use the K and Ka maps in separate combinations. In the case of the W band, four DA maps are available. We simply form an averaged map by taking two of them at a time, and we effectively form six DA maps. W_{ij} simply represents an averaged map obtained from the *i*th and *j*th DAs of the W band. (Other variations are possible, and we defer a more detailed discussion to a future publication; R. Saha et al. 2006, in preparation). In Table 1, we list all 48 possible linear combinations of the DA maps that lead to "cleaned" maps, C$\boldsymbol{i}$'s and CA$\boldsymbol{i}$'s, where $\boldsymbol{i} = 1, 2, \ldots, 24$.

Following the approach of Tegmark & Efstathiou (1996), we introduce a set of weights, $[\boldsymbol{W}_l] = (w_l^1, w_l^2, w_l^3, w_l^4)$, for each of the four DAs in the combination, and this defines our cleaned map as the linear combination

$$a_{lm}^{\rm clean} = \sum_{i=1}^{i=4} w_l^i \frac{a_{lm}^i}{B_l^i}, \qquad (1)$$

where a_{lm}^i is spherical harmonic transform of the map and B_l^i is the beam function for the channel *i* supplied by the *WMAP* team. The condition that the CMB signal remains untouched during cleaning is encoded as the constraint $[\boldsymbol{W}_l][\boldsymbol{e}] = [\boldsymbol{e}]^T[\boldsymbol{W}]^T = 1$, where $[\boldsymbol{e}]$ is a 4×1 column vector with unit elements.

Following Tegmark & Efstathiou (1996) and Tegmark et al. (2000, 2003), we obtain the optimum weights that combine four different frequency channels, subject to the constraint that the CMB is untouched, $[\boldsymbol{W}_l] = [\boldsymbol{e}]^T[\boldsymbol{C}_l]^{-1}/([\boldsymbol{e}]^T[\boldsymbol{C}_l]^{-1}[\boldsymbol{e}])$. Here the matrix $[\boldsymbol{C}_l]$ is

$$[\boldsymbol{C}_l] \equiv C_l^{ij} = \frac{1}{2l+1} \sum_{m=-l}^{m=l} \frac{a_{lm}^i a_{lm}^{j*}}{B_l^i B_l^i}. \qquad (2)$$

In practice, we smooth all the elements of the $\boldsymbol{C}_l$ using a moving average window over $\Delta l = 11$ before deconvolving by the beam function. This avoids the possibility of an occasional singular $\boldsymbol{C}_l$ matrix. The entire cleaning procedure is automated and takes approximately 3 hr on a 16 alpha processor machine to get the 48 cleaned maps. One of the cleaned maps, C8, is shown in Figure 1. In all 48 maps, some residual foreground contamination is visibly present along a small narrow strip on the Galactic plane. In a future publication, we will assess the quality of the foreground cleaning in these maps using the bipolar power spectrum method (Hajian & Souradeep 2003; Hajian et al. 2005; Hajian & Souradeep 2005), and we will compare them to other maps such as the internal Linear combination map of *WMAP*. For the angular power estimation that follows, the Kp2 mask employed suffices to mask the contaminated region in all 48 maps.

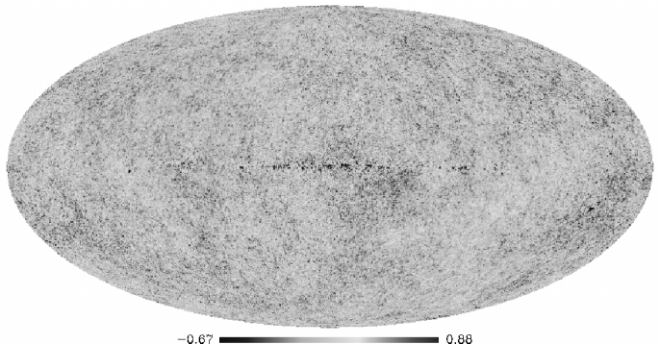

FIG. 1.—Cleaned map C8 for the K, Q2, V2, and W13 combination (in units of mK). The residual foreground contamination that is visible along the Galactic plane is well within the Kp2 mask that is applied before extracting the angular power spectrum. [*See the electronic edition of the Journal for a color version of this figure.*]

2.2. *Power Spectrum Estimation*

We obtain a cross-correlated power spectrum from these cleaned maps after applying a Kp2 mask. In choosing pairs C$\boldsymbol{i}$ and C$\boldsymbol{j}$ to be cross-correlated, we ensure that no DA is common between them. Figure 2 lists and plots the 24 cross-power spectra for which the noise bias is zero. The cross-power spectra are corrected for the effect of the mask, the beam, and the pixel window. These are accounted for by debiasing the pseudo-C_l estimate using the coupling (bias) matrix corresponding to the Kp2 mask and the appropriate circularized beam transform (Hivon et al. 2002). Figure 2 plots the 24 cross-power spectra (binned) individually. The spectra closely match each other for $l < 540$. The 24 cross-power spectra are then combined with equal weights into a single "uniform average" power spectrum.[3] We also estimate the residual power contamination in the uni-

[3] There exists the additional freedom to choose optimal weights for combining the 24 cross-power spectra that we do not discuss in this work.

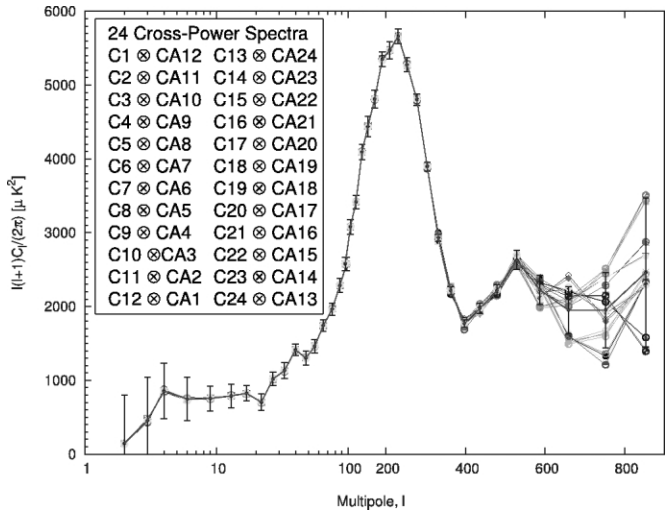

FIG. 2.—The 24 individual cross-power spectra corresponding to the cross-correlations listed in this figure are plotted. The cross spectra show a very small dispersion for $l \lesssim 540$. The average power spectrum is plotted using the gray line and gray error bars. The multipole range is on a log scale for $l < 100$ and is linear thereafter. [*See the electronic edition of the Journal for a color version of this figure.*]

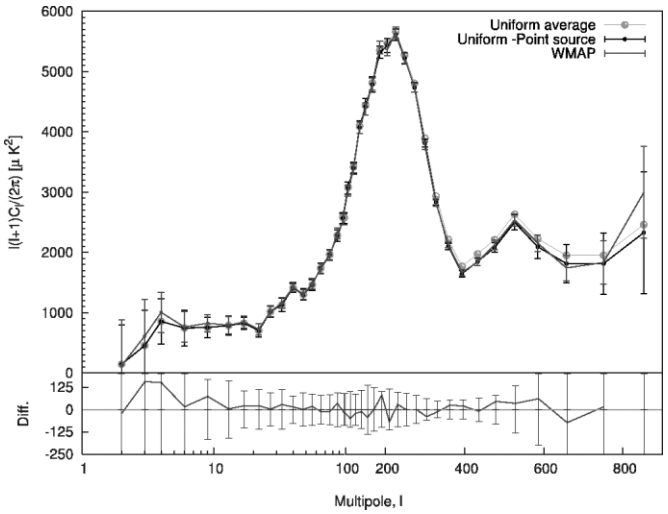

FIG. 3.—The uniform average power spectrum is plotted using the gray line. The black line shows the residual unresolved point-source–corrected power spectrum. The error bars are computed from the diagonal elements of the covariance matrix obtained from our simulation pipeline. Beyond $l = 400$, all the error bars are shifted by $\delta l = 10$ to visually distinguish between error bars obtained from our method and *WMAP*'s published error bars. The published binned *WMAP* power spectrum is plotted using the gray line with error bars. The multipole range $2 < l < 100$ is plotted in the log scale to show the small l behavior of the power spectrum. [*See the electronic edition of the Journal for a color version of this figure.*]

form average power spectrum from the unresolved point sources by running through our analysis the same source model used by the *WMAP* team to correct for this contaminant (Hinshaw et al. 2003b). The model is derived entirely within the *WMAP* data based on fluxes and spectra of 208 resolved point sources identified in the maps (Bennett et al. 2003b). The residual power from unresolved point sources is a constant offset of $\sim 140\ \mu\mathrm{K}^2$ for $l \gtrsim 400$ (and negligible at lower l). This residual is much less than the actual point-source contamination in the Q, Ka, or K band and is intermediate between the V- and W-band point-source contamination. It is noteworthy that the method significantly tempers the point-source residual at large l that otherwise is proportional to l^2 in each map. The final power spectrum is binned in the same manner as the *WMAP*'s published result for ease of comparison.

2.3. *Error Estimate on the Power Spectrum*

The errors on the final power spectrum are computed from 110 random Monte Carlo simulations of CMB maps for every DA, each with a realization based on a corresponding *WMAP* noise map (available at the Legacy Archive for Microwave Background Data Analysis [LAMBDA]) and on diffuse foreground contamination. The common CMB signal in all the maps was based on a realization of the *WMAP* "power-law" best-fit ΛCDM model (Spergel et al. 2003). We used the publicly available *Planck* Sky Model to simulate the contamination from the diffuse Galactic (synchrotron, thermal dust, and free-free) emission at the *WMAP* frequencies. The CMB maps were smoothed by the beam function appropriate for each of *WMAP*'s detectors. The set of DA maps corresponding to each realization was passed through the same pipeline that was used for the real data. Averaging over the 110 power spectra, we recover the model power spectrum, but with a hint of bias toward lower values in the low-l moments. For $l = 2$ and $l = 3$, the bias is -27.4% and -13.8%, respectively. However, this bias is negligible at higher l; e.g., at $l = 22$, it is only -0.8%.

The standard deviation obtained from the diagonal elements of the covariance matrix is used as the error bars on the C_l's obtained from the data. (The beam uncertainty is not included here but is deferred to future work in which we will also incorporate noncircular beam corrections; see Mitra et al. 2004.)

3. RESULTS

We obtain a uniform average power spectrum of the 24 cross-power spectra by following the method mentioned in § 2.2. The light gray line in Figure 3 compares our results with the *WMAP*-published power spectrum plotted with the gray line. The power spectra from two independent analyses are reasonably close. In case of a uniform average, a maximum difference of $92\ \mu\mathrm{K}^2$ is observed only for the octopole. For the large multipole range, the difference is small, and for $l = 752$ it is approximately $48\ \mu\mathrm{K}^2$. This is well within the $1\ \sigma$ error bar ($510\ \mu\mathrm{K}^2$) obtained from the simulation. The small but systematic excess at large multipoles is precisely resolved when our uniform average is corrected for the expected residual power from the unresolved point-source contamination described in §2.2. The point-source–corrected power spectrum is shown as the black line in this figure. The differences of this power spectrum with the published *WMAP* estimate are shown in the bottom panel of Figure 3. The differences are well within the $1\ \sigma$ error bars estimated from the simulations described in § 2.3.

We find a suppression of power in the quadrupole and octopole moments that is consistent with *WMAP*-published results. However, our quadrupole moment ($146\ \mu\mathrm{K}^2$) is a little larger than *WMAP*'s quadrupole moment ($123\ \mu\mathrm{K}^2$), and our octopole moment ($455\ \mu\mathrm{K}^2$) is less than *WMAP*'s octopole moment ($611\ \mu\mathrm{K}^2$). The uniform average power spectrum does not show the "bitelike" feature present in *WMAP*'s power spectrum at the first acoustic peak reported by *WMAP* (Hinshaw et al. 2003b). We perform a quadratic fit to the peaks and troughs of the binned

spectrum that is similar to *WMAP*'s analysis (Page et al. 2003). For the residual point-source–corrected (uniform average) power spectrum, we obtain the first acoustic peak at $l = 219.8 \pm 0.8$ (220.8 ± 0.8) with amplitude $\Delta T_l = 74.1 \pm 0.3$ μK (74.4 ± 0.3 μK), the second acoustic peak at $l = 544 \pm 17$ (545 ± 17) with amplitude $\Delta T_l = 48.3 \pm 1.2$ μK (49.6 ± 1.2 μK), and the first trough at $l = 419.2 \pm 5.6$ (418.7 ± 5.5) with amplitude $\Delta T_l = 41.7 \pm 1$ μK (42.2 ± 0.9 μK).

As cross-checks of the method, we have carried out analysis with other possible combinations of the DA maps:

1. The *WMAP* team also provide foreground-cleaned maps corresponding to Q1–W4 DAs (LAMBDA). The Galactic foreground signal, consisting of synchrotron, free-free, and dust emission, was removed using the three-band, five-parameter template-fitting method (Bennett et al. 2003b). We also include K- and Ka-band maps that are not foreground-cleaned. The resulting power spectrum from our analysis matches closely the uniform average power spectrum.
2. Excluding the K and Ka bands from our analysis, we get a power spectrum close to the uniform average results. Notably, we find a more prominent notch at $l = 4$ similar to *WMAP*'s published results.

This is a clear demonstration that the blind approach to foreground cleaning is comparable in efficiency to the approach using template-fitting methods and is certainly adequate for a reliable estimation of the angular power spectrum.

4. CONCLUSION

The rapid improvement in the sensitivity and resolution of the CMB experiments has imposed increasingly stringent requirements on the level of separation and removal of the foreground contaminants. Standard approaches to foreground removal usually incorporate the extra information about the foregrounds that is available at other frequencies and the spatial structure and distribution in constructing a foreground template at the frequencies of the CMB measurements. These approaches could be susceptible to the uncertainties and inadequacies of modeling that are involved when extrapolating from the frequency of the observation to CMB observations.

We carry out an estimation of the CMB power spectrum from the *WMAP* first-year data that is independent of the foreground model and that evades these uncertainties. The novelty is to make clean maps from the difference assemblies and to exploit the lack of noise correlation between the independent channels in order to eliminate noise bias. *This is the first demonstration that the angular power spectrum of CMB anisotropy can be reliably estimated with precision solely from the WMAP data (difference assembly maps) without recourse to any external data.*

The understanding of polarized foreground contamination in CMB polarization maps is rather scarce. Hence, modeling uncertainties could dominate the systematics error budget of conventional foreground cleaning. The blind approach extended to estimating polarization spectra after cleaning CMB polarization maps could prove to be particularly advantageous.

The analysis pipeline as well as the entire simulation pipeline are based on primitives from the HEALPix package.[4] We acknowledge the use of version 1.1 of the *Planck* reference sky model, prepared by the members of Working Group 2.[5] The entire analysis procedure was carried out at the IUCAA HPC facility. R. S. thanks the IUCAA for hosting his visits. We thank the *WMAP* team for producing excellent quality CMB maps and for making them available publicly. We thank Amir Hajian, Subharthi Ray, and Sanjit Mitra at IUCAA for helpful discussions. We are grateful to Lyman Page, Olivier Dore, Francois Bouchet, Simon Prunet, Charles Lawrence, and an anonymous referee for their thoughtful comments and suggestions on this work. P. J. and R. S. thank Sudeep Das for collaborating with them during the initial stages of this project.

[4] The HEALPix distribution is publicly available from the Web site http://healpix.jpl.nasa.gov/.

[5] Available at http://www.planck.fr/heading79.html.

REFERENCES

Bennett, C. L., et al. 2003a, ApJS, 148, 1
———. 2003b, ApJS, 148, 97
———. 2003c, ApJ, 583, 1
Bouchet, F. R., & Gispert, R. 1999, NewA, 4, 443
Dodelson, S. 1997, ApJ, 482, 577
Eriksen, H. K., et al. 2006, ApJ, 641, 665
Fosalba, P., & Szapudi, I. 2004, ApJ, 617, L95
Hajian, A., & Souradeep, T. 2003, ApJ, 597, L5
———. 2005, preprint (astro-ph/0501001)
Hajian, A., Souradeep, T., & Cornish, N. 2005, ApJ, 618, L63
Hinshaw, G., et al. 2003a, ApJS, 148, 63
———. 2003b, ApJS, 148, 135
Hivon, E., Górski, K. M., Netterfield, C. B., Crill, B. P., Prunet, S., & Hansen, F. 2002, ApJ, 567, 2
Hobson, M. P., Jones, A. W., Lasenby, A. N., & Bouchet, F. R. 1998, MNRAS, 300, 1
Jarosik, N., et al. 2003, ApJS, 145, 413
Limon, M., et al., eds. 2003, *Wilkinson Microwave Anisotropy Probe* (*WMAP*): Explanatory Supplement, Ver. 1.0 (Greenbelt: NASA/GSFC), http://lambda.gsfc.nasa.gov
Maino, D., Banday, A. J., Baccigalupi, C., Perrotta, F., & Górski, K. M. 2003, MNRAS, 344, 544
Maino, D., et al. 2002, MNRAS, 334, 53
Mather, J. C., Fixsen, D. J., Shafer, R. A., Mosier, C., & Wilkinson, D. T. 1999, ApJ, 512, 511
Mather, J., et al. 1994, ApJ, 420, 439
Mitra, S., Sengupta, A. S., & Souradeep, T. 2004, Phys. Rev. D, 70, 103002
Page, L., et al. 2003, ApJS, 148, 233
Patanchon, G., Cardoso, J.-F., Delabrouille, J., & Vielva, P. 2005, MNRAS, 364, 1185
Spergel, D. N., et al. 2003, ApJS, 148, 175
Tegmark, M. 1998, ApJ, 502, 1
Tegmark, M., de Oliveira-Costa, A., & Hamilton, A. J. 2003, Phys. Rev. D, 68, 123523
Tegmark, M., & Efstathiou, G. 1996, MNRAS, 281, 1297
Tegmark, M., Eisenstein, D. J., Hu, W., & Oliveira-Costa, A. 2000 ApJ, 530, 133